

Evaluation of solar wind-magnetosphere coupling functions during geomagnetic storms with the WINDMI model

E. Spencer,¹ A. Rao,¹ W. Horton,² and M. L. Mays²

Received 24 June 2008; revised 17 September 2008; accepted 3 November 2008; published 11 February 2009.

[1] We evaluate the performance of three solar wind-magnetosphere coupling functions in training the physics-based WINDMI model on the 3–7 October 2000 geomagnetic storm and predicting the geomagnetic *Dst* and AL indices during the 15–24 April 2002 geomagnetic storm. The rectified solar wind electric field, a coupling function by Siscoe, and a recent formula proposed by Newell are evaluated. The Newell coupling function performed best in both the training and prediction phases for *Dst* prediction. The Siscoe formula performed best during the training phase in reproducing the AL faithfully and capturing storm time events. The rectified driver was discovered to be the best in overall performance during both training as well as prediction phases, even though the other two coupling functions outperform it in the training phase. The results indicate that multiple drivers need to be concurrently employed in space weather models to yield different possible levels of geomagnetic activity.

Citation: Spencer, E., A. Rao, W. Horton, and M. L. Mays (2009), Evaluation of solar wind-magnetosphere coupling functions during geomagnetic storms with the WINDMI model, *J. Geophys. Res.*, 114, A02206, doi:10.1029/2008JA013530.

1. Introduction

[2] Prediction of the equatorial *Dst* index or auroral AE, AU, and AL indices from a magnetosphere-ionosphere model is often based on 1 hour ahead measurements of solar wind quantities made by the ACE (Advanced Composition Explorer) [Stone *et al.*, 1998] satellite at the Lagrangian L1 position. The measured values at ACE are the solar wind velocity along the sun earth line, the IMF strength, IMF angle and solar wind particle density in GSM coordinates. These quantities are combined to yield a solar wind-magnetosphere coupling function that can be used as inputs into a magnetosphere model. The outputs of the model are the predicted indices for up to 1 hour, which roughly corresponds to the time it takes for the solar wind to propagate from L1 to the nose of the magnetosphere.

[3] A precise formula for the solar wind-magnetosphere coupling function has not yet been agreed upon, although plenty of candidate functions exist [Newell *et al.*, 2007]. In magnetosphere models such as neural networks and nonlinear dynamical systems, variable parameters are tuned through training on geomagnetic storm data sets. It would appear advantageous for these models to use only one optimum coupling function to train and predict geomagnetic activity.

[4] Alternatively, concurrently trained models based on each coupling function can be implemented in parallel to predict different possibilities of geomagnetic activity. Some coupling functions may predict *Dst* better, while others may predict another index better. The idea of providing alternative predictions is then dependent upon evaluating the performance of each coupling function in the training of the model on a storm data set and in the prediction of different indices for a subsequent storm data set.

[5] In this work, we use three candidate solar wind-magnetosphere functions, based on earlier studies by Spencer *et al.* [2007], Mays *et al.* [2007], and Newell *et al.* [2007], to analyze two geomagnetic storm data sets. The coupling functions are used as inputs into a nonlinear physics model of the nightside magnetosphere called WINDMI. The outputs of the WINDMI model are the ring current energy which is considered to be proportional to the *Dst* index, and the region 1 field aligned current which is proportional to the AL index. The WINDMI model is trained using a large geomagnetic storm (minimum *Dst* of -180 nT) that occurred in the period of 3–7 October 2000. The parameter values obtained from the training phase are then used to evaluate the predictive performance of the WINDMI model for each of the candidate input functions on the 15–24 April 2002 geomagnetic storm, that had *Dst* minimums of -126 nT and -149 nT. The solar wind data for both storm periods contained ICME and interplanetary shock signatures [Mays *et al.*, 2007].

[6] The coupling functions used are (1) the rectified solar wind electric field [Reiff and Luhmann, 1986], (2) the coupling function proposed to Siscoe *et al.* [2002b], and (3) the coupling function proposed by Newell *et al.* [2007]. For this study, we do not use the other coupling functions in

¹Center for Space Engineering, Utah State University, Logan, Utah, USA.

²Institute for Fusion Studies, University of Texas, Austin, Texas, USA.

the work of *Newell et al.* [2007], since they were not found to correlate with the magnetic indices as well as the Newell formula. The rectified solar wind electric field is used as a baseline reference, as it is a well-known coupling function derived from basic physical principles.

[7] During the training phase, the parameters of the WINDMI model are optimized with a genetic algorithm (GA) with various cost functions that weight the importance of Dst and AL fits differently on the October 2000 storm. We optimized either the Dst performance exclusively, AL performance exclusively, or AL and Dst performance weighted equally. We also used another cost function that optimized the parameters to obtain periodic substorms in addition to good AL and Dst fits. The performance of each coupling function in the training phase is evaluated by observing how well the output indices approximates the measured indices, and whether key features of the October 2000 storm [*Mays et al.*, 2007] are captured.

[8] Next, with each optimized parameter set, we used the WINDMI model to predict the AL and Dst for the April 2002 storm. The performance of each function in the prediction phase is evaluated by how well the average relative variance (ARV) and correlation coefficient (COR) with the measured indices compare. The average relative variance gives a good measure of how well the optimized model predicts the future geomagnetic activity in a normalized mean square fit sense, while the correlation coefficient shows how well the model tracks the geomagnetic variations above and below its mean value.

[9] In section 2 we briefly describe the WINDMI model used in the forecasting of storms and substorms. In section 3, the solar wind-magnetosphere coupling functions used in this work are presented. In section 4, we explain the training techniques and give the forecasting results for the well known 15–24 April 2002 geomagnetic storm data set. In section 5, we make some conclusions and discuss future directions for this work.

2. WINDMI Model Description

[10] The plasma physics-based WINDMI model uses the solar wind dynamo voltage V_{sw} generated by a particular solar wind-magnetosphere coupling function to drive eight ordinary differential equations describing the transfer of power through the geomagnetic tail, the ionosphere and the ring current. The WINDMI model is described in some detail by *Doxas et al.* [2004], *Horton et al.* [2005] and more recently by *Spencer et al.* [2007]. The equations of the model are given by

$$L \frac{dI}{dt} = V_{sw}(t) - V + M \frac{dI_1}{dt} \quad (1)$$

$$C \frac{dV}{dt} = I - I_1 - I_{ps} - \Sigma V \quad (2)$$

$$\frac{3}{2} \frac{dp}{dt} = \frac{\Sigma V^2}{\Omega_{cps}} - u_0 p K_{\parallel}^{1/2} \Theta(u) - \frac{pVA_{eff}}{\Omega_{cps} B_{tr} L_y} - \frac{3p}{2\tau_E} \quad (3)$$

$$\frac{dK_{\parallel}}{dt} = I_{ps} V - \frac{K_{\parallel}}{\tau_{\parallel}} \quad (4)$$

$$L_I \frac{dI_1}{dt} = V - V_I + M \frac{dI}{dt} \quad (5)$$

$$C_I \frac{dV_I}{dt} = I_1 - I_2 - \Sigma_I V_I \quad (6)$$

$$L_2 \frac{dI_2}{dt} = V_I - (R_{pre} + R_{A2}) I_2 \quad (7)$$

$$\frac{dW_{rc}}{dt} = R_{pre} I_2^2 + \frac{pVA_{eff}}{B_{tr} L_y} - \frac{W_{rc}}{\tau_{rc}} \quad (8)$$

The largest energy reservoirs in the magnetosphere-ionosphere system are the plasma ring current energy W_{rc} and the geotail lobe magnetic energy W_m formed by the two large solenoidal current flows (I) producing the lobe magnetic fields.

[11] A second current loop is the I_1 R1 FAC current that is associated with the westward auroral electrojet. The field aligned current at the lower latitude that closes on the partial ring current is designated as I_2 . This current is only a part of the total region 2 FAC shielding current system.

[12] The current loops have associated voltages V and V_I driven by the solar wind dynamo voltage $V_{sw}(t)$. The resultant electric fields give rise to $\mathbf{E} \times \mathbf{B}$ perpendicular plasma flows. There is also parallel kinetic energy K_{\parallel} due to mass flows along the magnetic field lines.

[13] The high-pressure plasma trapped by the reversed lobe magnetic fields gives the thermal energy component $U_p = \frac{3}{2} p \Omega_{cps}$, where Ω_{cps} is the volume of the central plasma sheet.

[14] The nonlinear equations of the model trace the flow of electromagnetic and mechanical energy through eight pairs of transfer terms. The remaining terms describe the loss of energy from the magnetosphere-ionosphere system through plasma injection, ionospheric losses and ring current energy losses. The outputs of the model are the AL and Dst indices.

[15] The AL index from the model is obtained from the region 1 current I_1 by assuming a constant of proportionality $\lambda_{AL}[A/nT]$, giving $\Delta B_{AL} = -I_1/\lambda_{AL}$. The physics estimate of λ_{AL} from a strip approximation of the current I_1 gives a fixed scale between the current I_1 and the AL index. However an optimized linear scale yields better results of λ_{AL} than the fixed scale which does not take into account changes in width, height, and location of the electrojet during geomagnetic activity. The scaling factor for the 3–7 October 2000 storm was calculated to be 3275, while for the 15–24 April 2002 storm it was computed to be 2638, both in A/nT [*Spencer et al.*, 2007].

[16] The Dst signal from the model is given by ring current energy W_{rc} through the Dessler-Parker-Sckopke relation [*Dessler and Parker*, 1959; *Sckopke*, 1966].

$$Dst = -\frac{\mu_0}{2\pi} \frac{W_{rc}(t)}{B_E R_E^3} \quad (9)$$

where W_{rc} is the plasma energy stored in the ring current and B_E is the earth's surface magnetic field along the equator.

3. Solar Wind-Magnetosphere Coupling Functions

[17] The input into the WINDMI model is a voltage that is proportional to a combination of the solar wind parameters measured at L1 by the ACE satellite. These parameters are the solar wind velocity v_x , the IMF B_x^{IMF} , B_y^{IMF} , B_z^{IMF} , and the solar wind proton density n_{sw} , measured in GSM coordinates. The input parameters are time delayed to account for propagation of the solar wind to the nose of the magnetosphere at $10R_E$ as given by *Spencer et al.* [2007].

3.1. Rectified IMF Driver

[18] The first input function chosen for this study is the standard rectified vB_s formula [*Reiff and Luhmann, 1986*], given by

$$V_{sw}^{Bs} = 40(kV) + v_{sw} B_s^{IMF} L_y^{eff} (kV) \quad (10)$$

where v_{sw} is the x-directed component of the solar wind velocity in GSM coordinates, B_s^{IMF} is the southward IMF component and L_y^{eff} is an effective cross-tail width over which the dynamo voltage is produced. For northward or zero B_s^{IMF} , a base viscous voltage of 40 kV is used to drive the system.

3.2. Siscoe Driver

[19] The second input function is using a model given by *Siscoe et al.* [2002b], *Siscoe et al.* [2002a], and *Ober et al.* [2003] for the coupling of the solar wind to the magnetopause using the solar wind dynamic pressure P_{sw} to determine the standoff distance. This model includes the effects of the east–west component of the IMF through the clock angle θ_c . The Siscoe formula is given by

$$V_{sw}^S (kV) = 30.0(kV) + 57.6 E_{sw} (mV/m) P_{sw}^{-1/6} (nPa) \quad (11)$$

where

$$E_{sw} = v_{sw} B_T \sin(\theta_c/2) \quad (12)$$

is the solar wind electric field with respect to the magnetosphere and the dynamic solar wind pressure $P_{sw} = n_{sw} m_p v_{sw}^2$. Here m_p is the mass of a proton. The magnetic field strength B_T is the magnitude of the IMF component perpendicular to the x direction. The IMF clock angle θ_c is given by $\tan^{-1}(B_y/B_z)$. The solar wind flow velocity v_{sw} is taken to be approximately v_x . This voltage is described by *Siscoe et al.* [2002b] as the potential drop around the magnetopause that results from magnetic reconnection in the absence of saturation mechanisms.

3.3. Newell Driver

[20] The third input function is based on a recent formula from *Newell et al.* [2007, 2008] that accounts for the rate of

merging of the IMF field lines at the magnetopause. The Newell formula is given by

$$\frac{d\Phi_{MP}}{dt} = v_{sw}^{4/3} B_T^{2/3} \sin^{8/3}(\theta_c/2) \quad (13)$$

This formula is rescaled to the mean of equation (10) and given the same viscous base voltage of 40 kV. We obtain the rescaled Newell formula as,

$$V_{sw}^N = 40(kV) + \nu \frac{d\Phi_{MP}}{dt} \quad (14)$$

where ν is the ratio of the mean of the rectified voltage vB_s to the mean of $d\Phi_{MP}/dt$.

[21] In Figure 1, the three formulas are compared during the October 2000 geomagnetic storm. Since the rectified vB_s formula was used to normalize the Newell formula, there is a 10 kV difference at the baseline between these two formulas and the Siscoe input voltage.

[22] The rectified input can be seen to be the strongest driver, giving higher voltage peaks over most periods of the storm. Both the Siscoe voltage and the Newell voltage show their dependence on the IMF clock angle, most significantly noticeable on 4 October, the beginning of the sawtooth interval.

[23] The difference in the computed voltages during the 15–25 April storm period is shown in Figure 2. The significant differences in this period are that the rectified voltage can be seen to drop to the base viscous voltage of 40 kV very quickly in many intervals, again because of lack of IMF clock angle dependence. The rectified input also gives stronger peaks in value over the storm period.

4. Training and Prediction Performance

4.1. Technique

[24] For the purpose of performance evaluation on geomagnetic storm data sets, we used the October 2000 storm data as the training data set, and the April 2002 storm data as the prediction data set.

[25] To accomplish this, each input was used to analyze the October 2000 storm and the WINDMI model physical parameters optimized for that input against the measured AL and *Dst* indices. The best parameters found under a weighting scheme for a particular input were saved for use in the prediction phase.

[26] In the prediction phase, the parameters obtained under the different weighting schemes with a particular input were held fixed, and the predicted AL and *Dst* from the model driven by that input compared to the measured data.

[27] The Average Relative Variance (*ARV*) is used as a measure of performance for the goodness of fit between the WINDMI model output and the measured *AL* and *Dst* indices. The *ARV* is given by

$$ARV = \frac{\sum_i (x_i - y_i)^2}{\sum_i (\bar{y} - y_i)^2} \quad (15)$$

where x_i are model values and y_i are the data values. In order that the model output and the measured data are closely

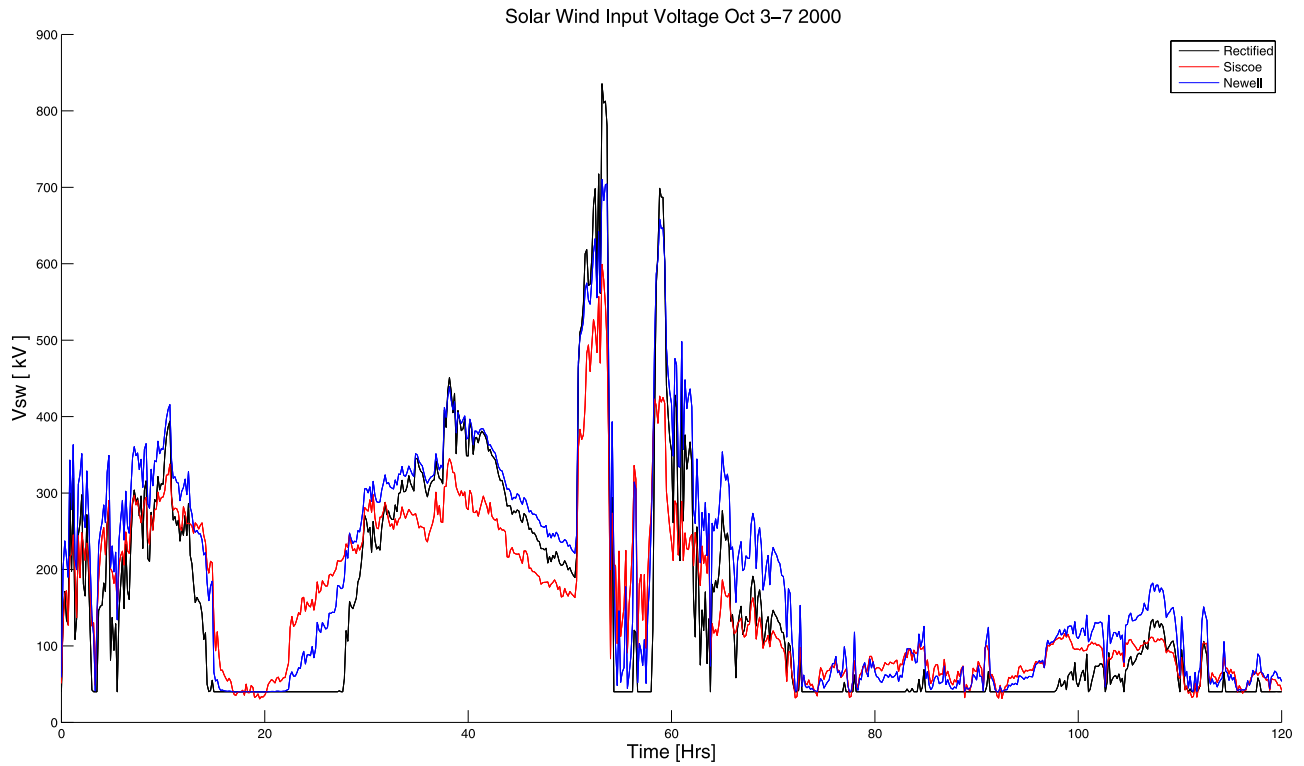


Figure 1. Comparison of the three coupling functions, V_{sw}^{Bs} , the rectified input, V_{sw}^S , the Siscoe-based input, and V_{sw}^N , the Newell input, calculated for 3-7 October 2000, a period of 120 hours.

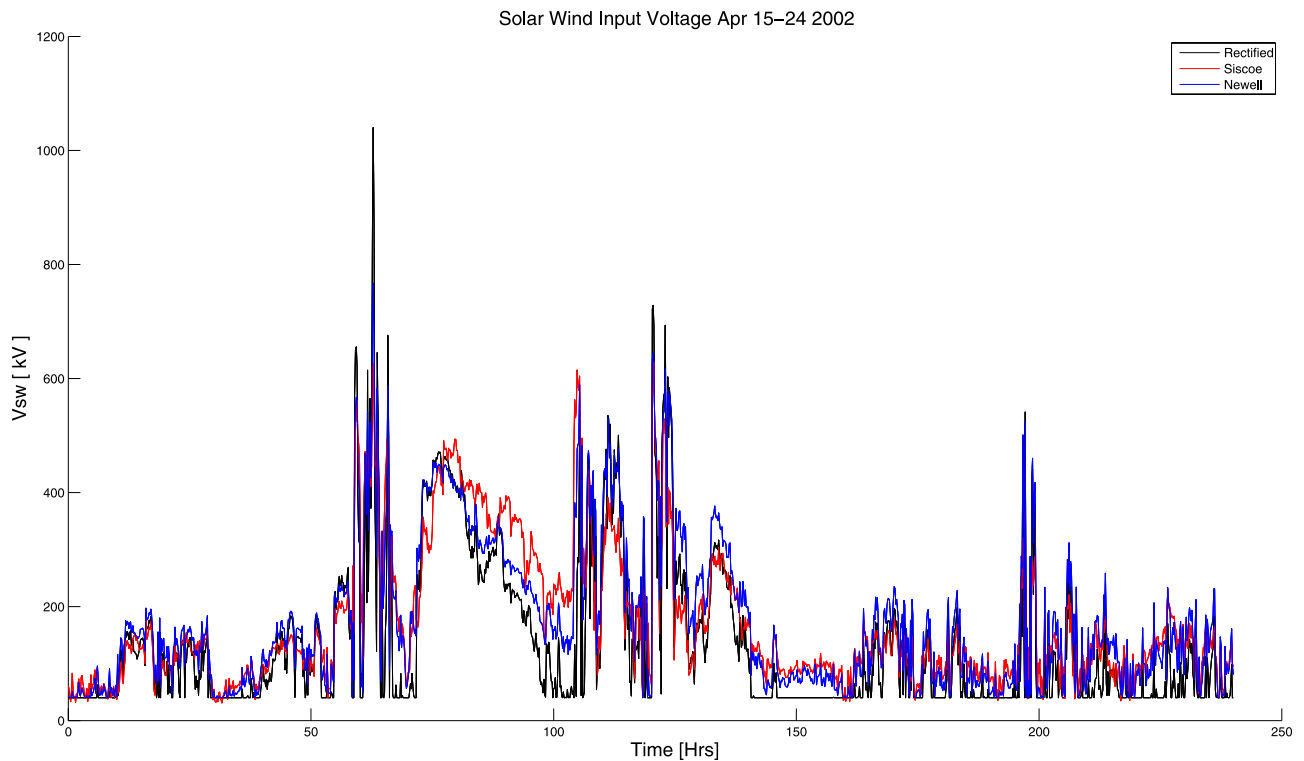


Figure 2. Comparison of the three coupling functions, V_{sw}^{Bs} , the rectified input, V_{sw}^S , the Siscoe-based input, and V_{sw}^N , the Newell input, calculated for 15-24 April 2002, a period of 240 hours.

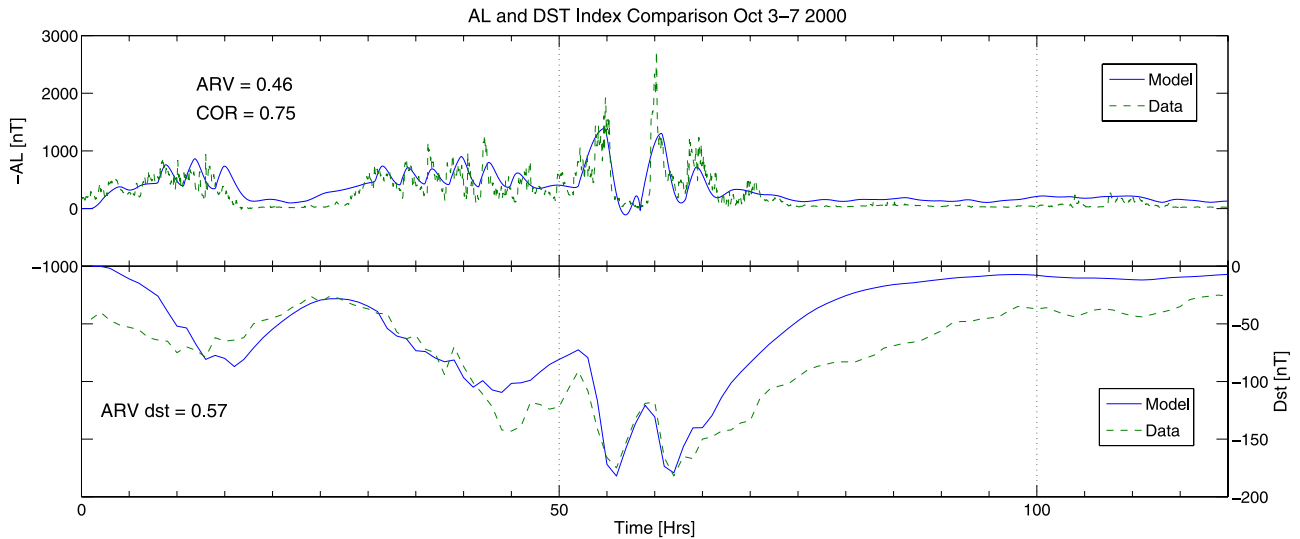


Figure 3. The best fit for 3–7 October 2000, obtained from the V_{sw}^S (Siscoe) input when optimizing against AL only in the training phase.

matched, ARV should be closer to zero. A model giving $ARV = 1$ is equivalent to using the average of the data for the prediction. If $ARV = 0$ then every $x_i = y_i$. ARV values above 0.8 are considered poor for our purposes. ARV below 0.5 is considered very good, and between 0.5 and 0.7 it is evaluated on the basis of feature recovery.

[28] The correlation coefficient COR is calculated against the AL index only as a measure of performance but not used as a cost function in the optimization process. COR is given by

$$COR = \frac{\sum_i (x_i - \bar{x})(y_i - \bar{y})}{\sigma_x \sigma_y} \quad (16)$$

COR is better the closer it is to 1. It indicates anticorrelation if the value is close to -1 . σ_x and σ_y are the model and data variances respectively. Typically, if the correlation coefficient

is above 0.7 the performance is considered satisfactory for the physics-based WINDMI model.

[29] The ARV and COR values are calculated over the period when the most geomagnetic activity occurs. For the 3–7 October 2000 storm this was between hour 24 to hour 72 over the 120 hour storm period. For the 15–24 April storm, the ARV and COR was calculated from hour 48 to 144 out of the 240 hours total storm period.

4.2. Results

4.2.1. Training the Model

[30] In the training phase, we first optimized the WINDMI model parameters for a best match to the AL index for the October 2000 storm. It was found that the Siscoe input, V_{sw}^S , not only gave the best fit (ARV 0.46, COR 0.75), but was also the only input that was able to reproduce some of the sawtooth oscillations that occurred on 4 October. This result is shown in Figure 3. The Dst

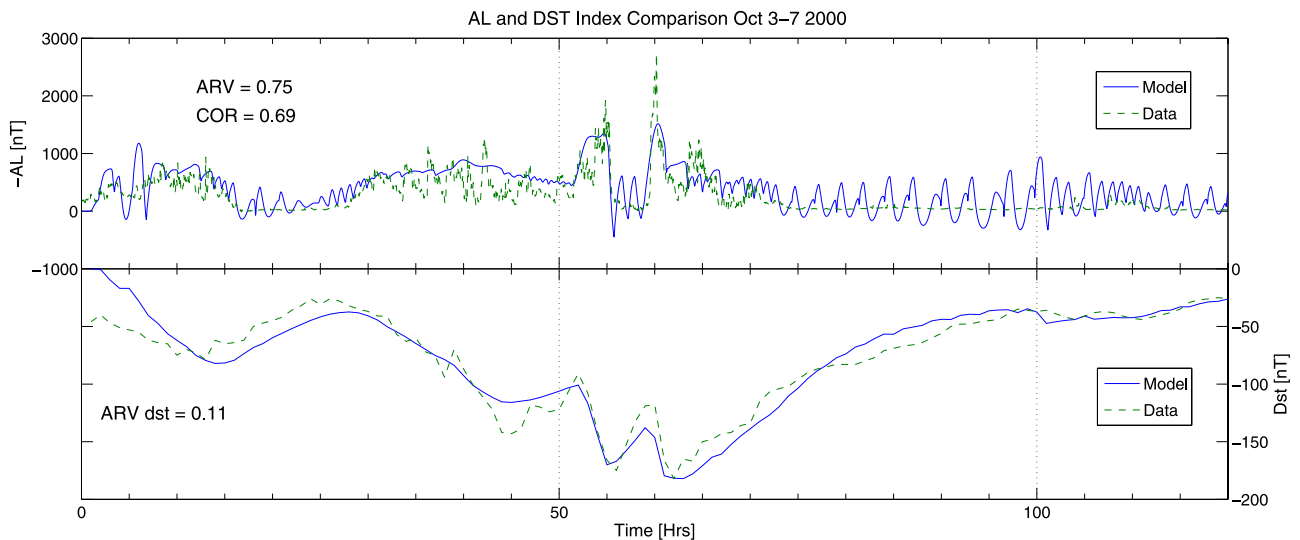


Figure 4. The best fit for 3–7 October 2000, obtained from the V_{sw}^N (Newell) input when optimizing against Dst only in the training phase.

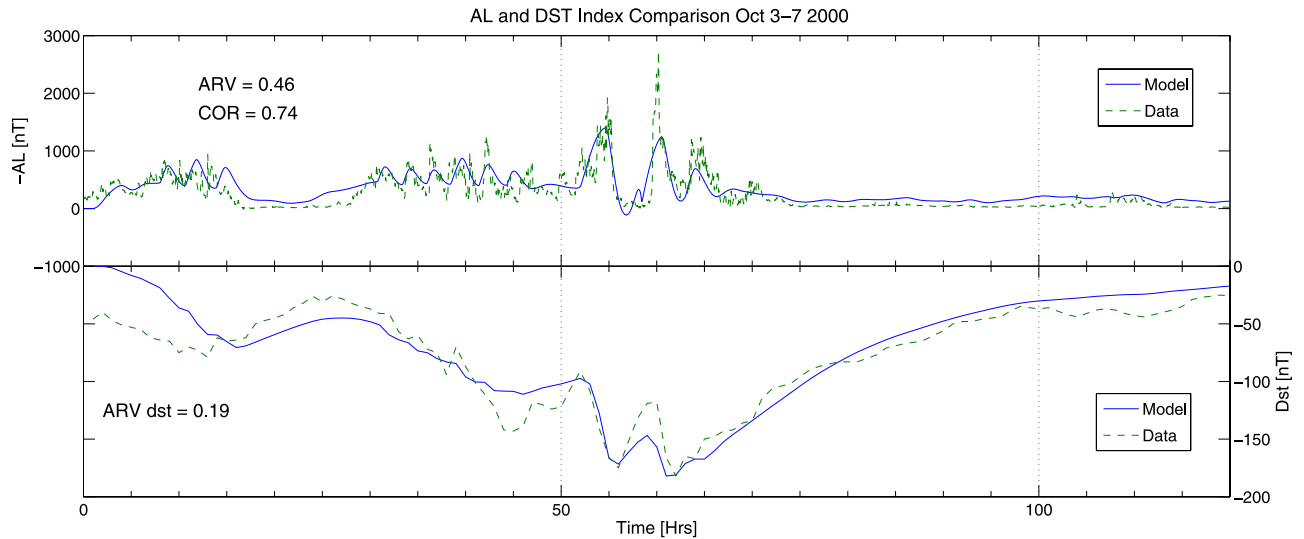


Figure 5. AL and Dst for 3–7 October 2000 obtained using the Siscoe input with equal weighting given to AL and Dst for the training phase.

match was also best with the Siscoe input, with an ARV of 0.57.

[31] When we optimized against the Dst index only, we found that the Newell input, V_{sw}^N performed best (ARV = 0.11). All three inputs performed poorly on AL under this optimization criterion, but this was only to be expected, since the AL index represents short timescale variations while the Dst is more representative of overall energy in the ring current which varies on a longer timescale of several hours.

[32] The result obtained when optimizing against Dst only with the Newell input is shown in Figure 4. We observe that the AL fit is poor in terms of features, as well as the ARV measure. Because of the very poor AL performance, the optimized parameters in this case were not used in the prediction phase.

[33] We then turned to optimizing the model against AL and Dst equally. Here we found that the Siscoe input performed best, with an ARV of 0.46, equal to what was obtained when it was optimized against AL only, but now with a markedly improved Dst fit (ARV = 0.19). The result is shown in Figure 5. The Newell input was next in quality of performance, and the rectified input V_{sw}^{Bs} performed the poorest. The results obtained when optimizing against AL and Dst equally are summarized in Table 1.

[34] We note that when we optimized the model with the additional criteria of fitting oscillations of 2–3 hour interval on 4 October, the Siscoe input still performed best. However these results did not differ significantly in ARV and

COR values from the results obtained when optimized with equal weighting of AL and Dst .

[35] The results in the training phase indicated that the Siscoe input was the best one to use if we wanted to obtain the storm time features accurately. However the prediction phase indicated rather differently, which we discuss next.

4.2.2. Prediction Phase

[36] In this phase, we used the parameters of the model obtained under the different criteria to see how well the model would reproduce the features of the 15–24 April 2002 storm, and how good the ARV and COR measures were.

[37] When we used the parameters from optimization against AL alone, the best prediction was obtained using the Newell input, which gave an ARV of 0.56 for AL. The Dst fit was with an ARV of 0.26.

[38] The best overall prediction was expected from the parameters obtained when optimizing against both the AL and the Dst weighted equally. The prediction results are summarized in Table 2. The unexpected result here was that the rectified input, V_{sw}^{Bs} , which did not perform as well as the Siscoe and Newell inputs in the training phase, was better in the overall prediction of the AL and Dst indices for the April 2002 storm, with a correlation coefficient COR of 0.72 against AL.

[39] In Figure 6, we observe that the rectified input can predict the long timescale variations in the AL index (ARV = 0.63), and also predicts the Dst variation with some accuracy (ARV = 0.23). It was unable however to produce the sawtooth oscillations that occurred on 18 April 2002.

Table 1. Training Results for October 2000 When Optimizing Against AL and Dst Weighted Equally

| Storm OCT 2000, Training Phase | | | |
|--------------------------------|--------|---------|--------|
| Input | AL ARV | DST ARV | AL COR |
| Rectified | 0.57 | 0.28 | 0.67 |
| Siscoe | 0.46 | 0.19 | 0.74 |
| Newell | 0.51 | 0.2 | 0.73 |

Table 2. Prediction Results for April 2002 Using Parameters From Optimization Against AL and Dst Weighted Equally

| Storm APR 2002, Prediction Phase | | | | |
|----------------------------------|--------|---------|--------|-------------|
| Input | AL ARV | DST ARV | AL COR | Dir. AL COR |
| Rectified | 0.63 | 0.23 | 0.72 | 0.62 |
| Siscoe | 1.2 | 0.39 | 0.47 | 0.55 |
| Newell | 0.8 | 0.21 | 0.59 | 0.68 |

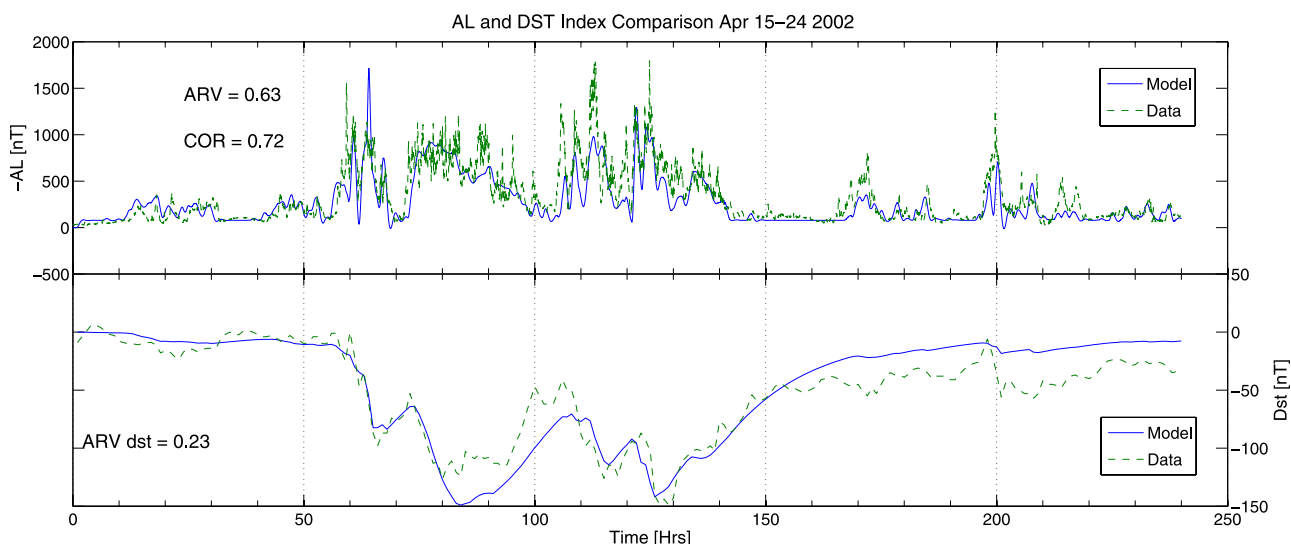


Figure 6. The 15–24 April 2002 prediction using V_{sw}^{Bs} (rectified) with optimized parameters from equal weighting of AL and *Dst*.

[40] Figure 7 shows that the Newell input does marginally better on the *Dst* prediction (ARV 0.21), but does not do nearly as well as the rectified input with the AL index prediction.

[41] The final column in Table 2 shows the direct correlation between the calculated input and the AL index during the prediction phase. When the direct correlation is calculated for the training phase, the WINDMI model always does better than a direct correlation, which is clearly expected since the model is tuned to the data set using the optimization process. The *Dst* index is also better with the model, since it represents the energy in the ring current which can only be obtained from the inputs through weighted time integration.

[42] In the prediction phase, the *Dst* is still better with the model, but direct correlation between the calculated inputs and the AL index outperforms the model predictions for

both the Newell and Siscoe formulas. Again, the rectified input used with the WINDMI model does best, with COR of 0.72 compared to a direct correlation of 0.62.

[43] Although the Siscoe input performed best during the training phase, it performed poorly in the prediction phase. The Newell input consistently produced better *Dst* ARV figures, both in training as well as in prediction, but was not as good in AL during the training phase compared to the Siscoe input, and not as good in AL as the rectified input during the prediction phase. The rectified input appeared to be the most reliable input to use for AL prediction.

5. Discussion and Conclusions

[44] Our investigation indicates that although the rectified vB_s is not an accurate input for the analysis of feature reproduction capability of the WINDMI model in a geo-

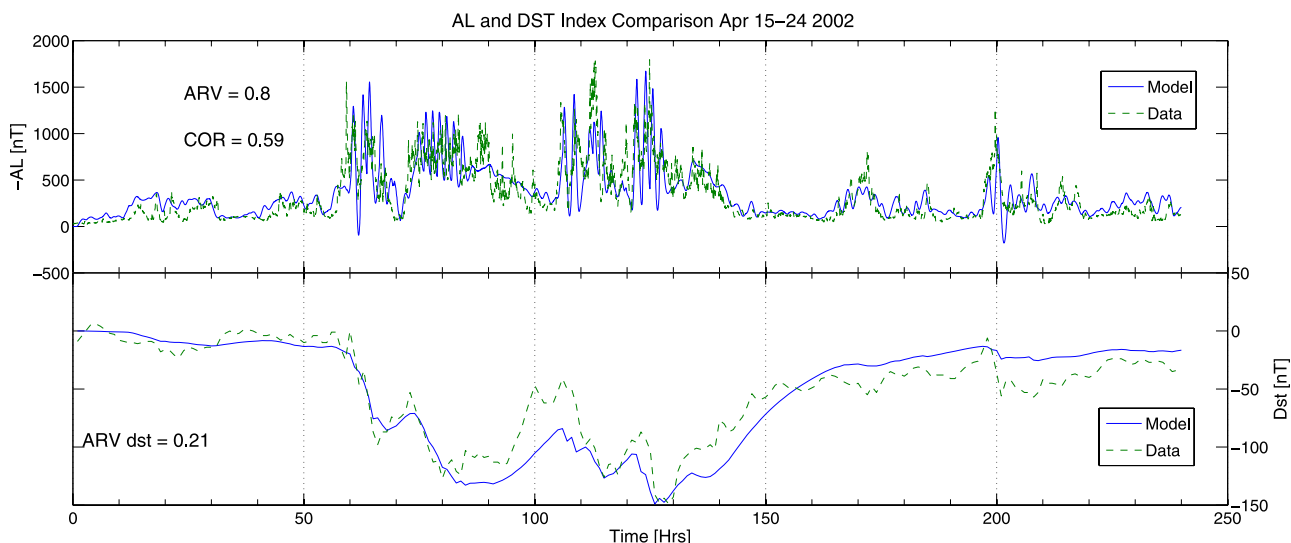


Figure 7. The 15–24 April 2002 prediction using V_{sw}^N (Newell) with optimized parameters from equal weighting of AL and *Dst*.

magnetic storm, it is a robust driver compared to other more refined inputs such as the Newell or Siscoe drivers. We interpret this as a result of the variability of the state of the magnetosphere.

[45] With inputs such as the Siscoe or Newell drivers that account for more physics, the optimization process constrains the physical state of magnetosphere more accurately during a particular storm such as the October 2000 event. However, since the state of the magnetosphere is different during April 2002, the prediction results using the magnetosphere structure of an earlier storm becomes unreliable.

[46] The rectified driver, although crude, appears to optimize the physical state of the magnetosphere in a more average manner. This state is therefore robust enough to be used as a predictor for future events.

[47] Our results also show that it may be necessary to use different drivers to predict different indices better. The Newell input produced the best *Dst* fits during the training as well as the prediction phases. Thus it may be better to use this input when needing a good *Dst* prediction, even though the AL is predicted better by the rectified driver.

[48] The Siscoe input can still be used for post storm analysis to determine the physical state of the magnetosphere a little more accurately. It is also possible that if the Siscoe input were used in real time with the optimization of the parameters performed closer to the time of the storm, it may yield better prediction results. This is a subject for future investigation.

[49] Hereafter, we will use all three of these drivers in a real time prediction system <http://orion.ph.utexas.edu/~windmi/realtime/> of the AL and *Dst* index, running three parallel WINDMI model instances, in order to give three possible sets of predicted indices. The three models will be optimized concurrently every 8 to 12 hours, with the AL and *Dst* weighted equally. At this time this appears to be the most reliable configuration to give a one hour ahead prediction of the AL and *Dst* index during geomagnetic storms.

[50] **Acknowledgments.** This work was partially supported by the National Science Foundation under the NSF grants ATM-0720201 and ATM-0638480. The solar wind plasma and magnetic field data were obtained from ACE instrument data at the NASA CDA Web site. The geomagnetic indices used were obtained from the World Data Center for Geomagnetism in Kyoto, Japan.

[51] Amitava Bhattacharjee thanks the reviewers for their assistance in evaluating this paper.

References

- Dessler, A., and E. N. Parker (1959), Hydromagnetic theory of geomagnetic storms, *J. Geophys. Res.*, *64*(12), 2239–2259.
- Doxas, I., W. Horton, W. Lin, S. Seibert, and M. Mithaiwala (2004), A dynamical model for the coupled inner magnetosphere and tail, *IEEE Trans. Plasma Sci.*, *32*(4), 1443–1448.
- Horton, W., M. Mithaiwala, E. Spencer, and I. Doxas (2005), WINDMI: A family of physics network models for storms and substorms, in *Multi-Scale Coupling of Sun-Earth Processes*, edited by A. Lui, Y. Kamide, and G. Consolini, pp. 431–436, Elsevier, New York.
- Mays, M. L., W. Horton, J. Kozyra, T. H. Zurbuchen, C. Huang, and E. Spencer (2007), Effect of interplanetary shocks on the AL and *Dst* indices, *Geophys. Res. Lett.*, *34*, L11104, doi:10.1029/2007GL029844.
- Newell, P., T. Sotirelis, K. Liou, C.-I. Meng, and F. Rich (2007), A nearly universal solar wind-magnetosphere coupling function inferred from 10 magnetospheric state variables, *J. Geophys. Res.*, *112*, A01206, doi:10.1029/2006JA012015.
- Newell, P., T. Sotirelis, K. Liou, and F. Rich (2008), Pairs of solar wind-magnetosphere coupling functions: Combining a merging term with a viscous term works best, *J. Geophys. Res.*, *113*, A04218, doi:10.1029/2007JA012825.
- Ober, D. M., N. C. Maynard, and W. J. Burke (2003), Testing the Hill model of transpolar potential saturation, *J. Geophys. Res.*, *108*(A12), 1467, doi:10.1029/2003JA010154.
- Reiff, P. H., and J. G. Luhmann (1986), Solar wind control of the polar-cap voltage, in *Solar Wind-Magnetosphere Coupling*, edited by Y. Kamide and J. A. Slavin, pp. 453–476, Terra Sci., Tokyo.
- Skopke, N. (1966), A general relation between the energy of trapped particles and the disturbance field near the Earth, *J. Geophys. Res.*, *71*(13), 3125–3130.
- Siscoe, G. L., N. U. Crooker, and K. D. Siebert (2002a), Transpolar potential saturation: Roles of region-1 current system and solar wind ram pressure, *J. Geophys. Res.*, *107*(A10), 1321, doi:10.1029/2001JA009176.
- Siscoe, G. L., G. M. Erickson, B. U. O. Sonnerup, N. C. Maynard, J. A. Schoendorf, K. D. Siebert, D. R. Weimer, W. W. White, and G. R. Wilson (2002b), Hill model of transpolar potential saturation: Comparisons with MHD simulations, *J. Geophys. Res.*, *107*(A6), 1075, doi:10.1029/2001JA000109.
- Spencer, E., W. Horton, L. Mays, I. Doxas, and J. Kozyra (2007), Analysis of the 3–7 October 2000 and 15–24 April 2002 geomagnetic storms with an optimized nonlinear dynamical model, *J. Geophys. Res.*, *112*, A04S90, doi:10.1029/2006JA012019.
- Stone, E. C., A. M. Frandsen, R. A. Mewaldt, E. R. Christian, D. Margolies, J. F. Ormes, and F. Snow (1998), The advanced composition explorer, *Space Sci. Rev.*, *86*, 1–22.

W. Horton and M. L. Mays, Institute for Fusion Studies, University of Texas, RLM 11.222, Austin, TX, USA.

E. Spencer and A. Rao, Center for Space Engineering, Utah State University, EL241C Logan, UT 84322, USA. (espcencer@engineering.usu.edu)